

Tunable Infrared Pixels via Monolithically Integrated Dynamic Graphene Metasurfaces

Thomas E. Beechem*, Michael D. Goldflam*, Isaac Ruiz*, Stephen W. Howell†, Michael B. Sinclair*, Anna Tauke-Pedretti*, Joel R. Wendt*, Evan M. Anderson*, Wesley Coon*, Torben R. Fortune*, Sam Hawkins*, Patrick Finnegan*, Clark Kadlec*, Preston Webster*, Eric A. Shaner*, John Klem*, Jin K. Kim* and David W. Peters*

*Sandia National Laboratories, Albuquerque, NM 87185

†Naval Surface Warfare Center, Crane, IN 47522-5001

Email: tebeeche@sandia.gov

Abstract—Long-wave infrared (LWIR) pixels exhibiting dynamic, real-time, spectral tunability were designed, fabricated, and tested. The pixels are composed of a type-II superlattice detector that is monolithically integrated with a graphene enabled tunable metasurface. The combined detector and filter operate as a single solid state device with no moving parts whose alignment is implicit with fabrication. Functionally, tunability results from the plasmonic properties of graphene that are acutely dependent upon the carrier concentration within the infrared. Voltage induced changes in graphene’s carrier concentration can thus be leveraged to change the metasurface’s transmission thereby altering the “colors” of light reaching the broadband detector and hence its spectral responsivity. These characteristics were practically demonstrated by measuring the spectral responsivity of the detector at varying levels of bias across the graphene where relative changes in excess of 20% were observed as a result of spectral shifts in the filter of nearly 50 cm^{-1} at $\sim 1000\text{ cm}^{-1}$. Taken in total, the effort serves as a proof of concept for spectrally agile infrared detection offering the potential of independent pixel to pixel spectral tunability.

Keywords—infrared; detection; graphene; metasurface

I. INTRODUCTION

Infrared (IR) sensors image scenes that are spatially, spectrally, and temporally dynamic even as the pixels themselves are comparatively inflexible. These pixels are typically composed of complex semiconductors like HgCdTe (MCT) and InGaAs that are utilized both as a consequence of their bandgap being commensurate with IR wavelengths and the ability to vary this gap over a spectral range based upon the material’s composition. Such tunability is realized, however, only during design as composition—and hence spectral responsivity—is fixed upon fabrication.

For this reason, dynamic, real-time, tunability has been achieved only by external means through the use of filter wheels, tunable filters, or interferometry.[1] These solutions fundamentally lack for two reasons, however. First, they are decoupled from the detector and thus require both alignment and an increase the size of the optical set-up. Second, each of these approaches filters the light uniformly over the entire

array. It is thus impossible to assess differing portions of a scene simultaneously with separate spectral bands. Overcoming these constraints necessitates a pixel that is itself as dynamic as the scene it is tasked to image.

Tunable pixels can be realized using two broad approaches. First, the detector can be constructed out of materials whose optical properties can be controllably varied. Bilayer graphene[2] and InAs[3] quantum dots have each been used to this end but have yet to achieve responsivities comparable to more traditional architectures. Alternatively, a broadband detector can be placed “behind” a tunable filter that is registered at the single pixel level. This is the approach taken here.

Tunable infrared filters have recently emerged as an increasingly common technology all their own. Devices have been demonstrated leveraging phenomena ranging from phase change[4] and mechanical movement[5] to plasmonic excitation.[6] Regardless of phenomena, tunable filters operate by attempting to maximize field concentration within a material whose optical properties are controllably varied. This is most often achieved using patterned metasurfaces that functionally act to enhance the field within the tunable material. The tunable material, meanwhile, is actuated with an electrical bias to either change shape (SiN), phase (*e.g.*, via Joule-heating in GST,VO₂), or the free carrier concentration (CdO, graphene).

These tuning approaches naturally offer trade-offs. Electromechanical and phase change produce larger tuning ranges than altering the carrier concentration. Changing shape necessitates moving parts, however. Phase change requires Joule-heating, which limits the effectiveness of the cooled detector sitting behind it. Modulating charge carriers, in contrast, minimally dissipates power and is extremely fast. Furthermore, being the basis of semiconductor technology, these approaches possess an architecture whose integration atop an imaging array could be most benign.

To demonstrate, tunable graphene filters were fabricated directly atop a gallium-free type-II superlattice (T2SL) detector with a cut-off wavelength of $11\ \mu\text{m}$. Graphene is chosen for two reasons. First, it has been used in numerous “stand-

DISTRIBUTION STATEMENT A. Approved for public release: distribution is unlimited.

alone” tunable infrared filters reported previously.[6] Second, being a two-dimensional van Der Waals solid, graphene can be transferred at room temperature directly atop the detector material stack while imparting virtually no mechanical load. The filter can thus be made directly atop the pixel using typical lithography approaches without damaging the sensing element in any way. The finished pixel is thus composed of a tunable filter that is fully integrated to the detector as a single solid state device.

The following describes the architecture and operation of this tunable integrated pixel (TIP). Specifically, spectral responsivity of the TIP-device was measured as a function of electrostatic gating of the graphene filter. Dynamic and continuous tuning of the relative spectral responsivity resulting in changes of $> 20\%$ were observed. These changes were then leveraged to dynamically alter the comparative sensitivity between two spectrally separated bands of polypropylene to emphasize the device’s “push-button” tunability. Taken together, the effort serves as a proof of principle demonstration highlighting a path towards independent spectral tuning of individual pixels across an array.

RESULTS

The fabricated tunable integrated pixel (TIP) is shown in Figure 1 from both a plan and cross-sectional view. Beginning from the top, the filter is composed of a Au grating metasurface that excites the graphene plasmon. The graphene plasmon’s energy—and hence the pass-band of the filter—is controlled dynamically by placing a voltage across a thin HfO_2 layer that rests above the graphene using the Au. The voltage electrostatically dopes the graphene inducing changes in the material’s optical properties and thus its plasmonic response. A thick Al_2O_3 layer supports the graphene and practically serves as a “coarse knob” for dictating the static spectral character of the filter.[7] Each of these layers is fabricated atop the detector through either layer transfer techniques (graphene) or atomic layer deposition (ALD). Processing did not appreciably change the detector properties.

The detector is composed of a gallium-free type-II superlattice (T2SL) long-wave infrared (LWIR) absorber synthesized atop a GaSb substrate. Use of a T2SL detector is motivated by theoretical predictions of dark current characteristics surpassing that of mercury cadmium telluride (MCT) [8], [9], [10], [11]. It is important to note that while a T2SL was selected for use in this work, the tunable architecture employed here is absorber material agnostic meaning that it could easily be applied atop a conventional MCT detector yielding a significant increase in quantum efficiency over that of the T2SL. For the present case, quantum efficiency is hindered by the low absorption coefficient of the $\sim 2 \mu\text{m}$ thick superlattice in the LWIR wavelength range [12], [13].

The tunable integrated pixel was characterized initially *via* measurements of its spectral responsivity. These measurements were carried out by focusing light output from a Fourier transform infrared spectrometer (FTIR) onto the device. The electrical output of the detector was then fed directly back

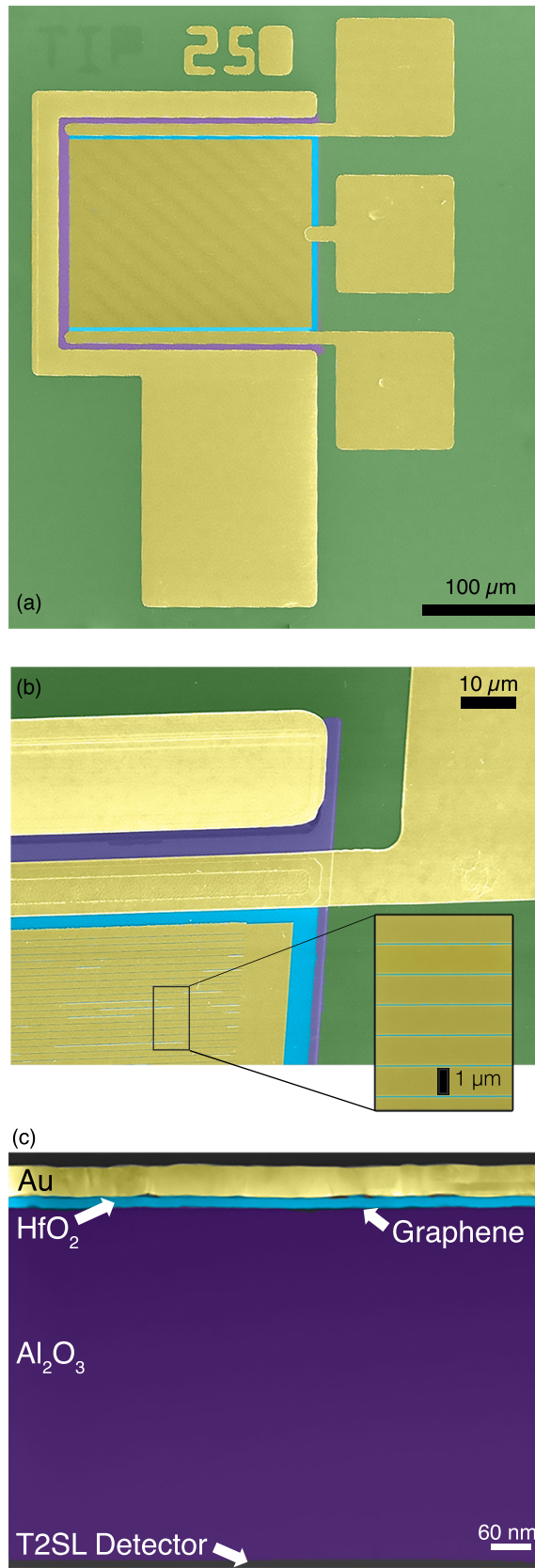


Fig. 1. False color micrographs of tunable integrated pixel from (a,b) plan and (c) cross-sectional views. Inset of (b) presents a detailed view of the nanoantenna filter consisting of a metallic grating sitting atop a thin HfO_2 dielectric and graphene stack.

into the FTIR such that the response from $\sim 8\text{-}12\ \mu\text{m}$ ($800\text{-}1200\ \text{cm}^{-1}$) could be assessed continuously as a function of filter bias. Spectral characteristics of the light-source were calibrated using a commercial DTGS detector.[14]

Spectral tuning of the device is apparent, repeatable, and continuous as shown in Figure 2. Quantitatively, the detector's relative response changes by nearly $\pm 20\%$ relative to that at the charge neutrality point (CNP) of the graphene. The location of maximum responsivity, meanwhile, varies by $\sim 50\ \text{cm}^{-1}$. The changes are analog allowing for continuous tuning as opposed to the digital states typically available when filtering with phase change materials.

Variations in the spectral response are caused by changes in the amount of transmitted light through the filter rather than a spurious alteration in the detector's charge transport induced by the electrostatic gating of the graphene. This is evidenced by comparing the current-voltage characteristics of the graphene with the spectral response of the detector at $1200\ \text{cm}^{-1}$ as shown in Figure 2(c). Specifically, changes in spectral responsivity of the TIP device as a whole qualitatively match the amount of current moving through the graphene. This correlation, in combination with changes observed in the device's reflectance as a function of gate voltage (not shown), indicates that the graphene/dielectric stack is operating as a tunable light filter.

The tunability of the graphene filter allows for "push-button" control of a pixel's spectral sensitivity. To demonstrate, a thin polypropylene film was placed between the light source and the TIP device. The infrared spectrum measured by the TIP pixel was then acquired with the graphene set at several different Fermi-levels (ϵ_f) as controlled by the gate voltage. Results are shown in Figure 3 where changes in the response—and hence sensitivity to—certain modes are appreciably varied. This is exemplified by comparing the signals near 930 and $1100\ \text{cm}^{-1}$. For the lower energy mode, maximum sensitivity (*i.e.*, largest "dip" in signal) is observed when the graphene Fermi-level is maximized—*i.e.*, the optical conductivity of graphene is greatest. The opposite is true for the mode near $1100\ \text{cm}^{-1}$ leading to difference spectra that "flip" in the magnitude of their signal near $1000\ \text{cm}^{-1}$ (see Figure 3(b)). Effectively, the device is more sensitive to one mode as it becomes less sensitive to another. This spectral selectivity is typically acquired through the use of stand-alone filters. Here, it is being demonstrated as part of the detector itself.

The filter operates electrostatically with minimal dissipation of current. Here, we have monitored the graphene current as a means to correlate changes in the graphene with that of the spectral response. For practical use, this monitoring is unnecessary. The filter dissipates only the current "leaking" through the gate, which is orders of magnitude less than that moving through the detector itself. The TIP device therefore provides additional functionality with minimal additional power consumption.

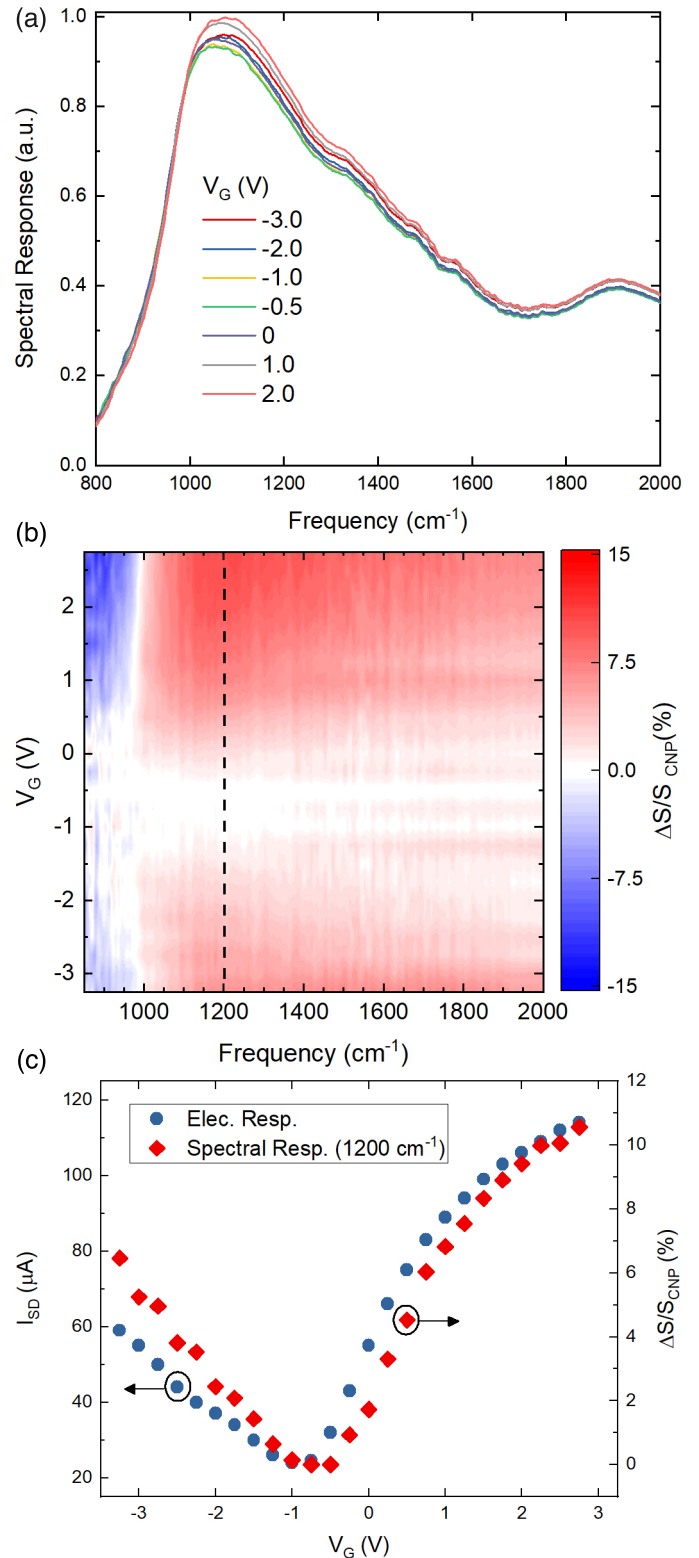


Fig. 2. (a) Spectral photoresponse of TIP device at varying gate voltages used to control spectral response of filter. (b) Map of spectral responsivity as a function of wavelength and gate voltage. Plots in (a) are horizontal line cuts of (b). (c) Comparison of electrical transport within the graphene filter and the TIP spectral responsivity at $1200\ \text{cm}^{-1}$ (vertical dashed line in (b)).

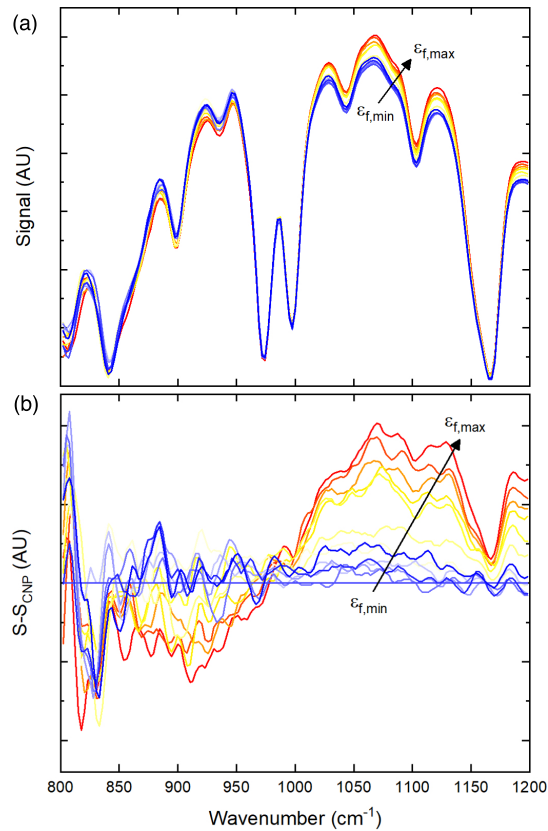


Fig. 3. (a) Measured and (b) difference spectra of polypropylene from the TIP-device as the Fermi-level (ϵ_f) of the graphene is changed via the gate voltage.

CONCLUSIONS

By fabricating a dynamic graphene metasurface atop a T2SL infrared detector, tunable spectral responsivity at the single pixel level was demonstrated in the LWIR. The monolithic approach increases functionality while maintaining the standard lamellar architecture of semiconductor devices without appreciably increasing the size or power consumption of the detector. With this demonstration, a path towards imaging arrays exhibiting pixels with independent and controllable spectral responsivities is identified.

ACKNOWLEDGMENT

This work was supported by the Laboratory Directed Research and Development (LDRD) program at Sandia National Laboratories. Sandia National Laboratories is a multimission laboratory managed and operated by National Technology and Engineering Solutions of Sandia LLC, a wholly owned subsidiary of Honeywell International Inc. for the U.S. Department of Energy's National Nuclear Security Administration under contract DE-NA0003525.

REFERENCES

- [1] C. D. Tran, "Infrared multispectral imaging: Principles and instrumentation," *APPLIED SPECTROSCOPY REVIEWS*, vol. 38, no. 2, pp. 133–153, 2003.
- [2] J. Yan, M. Kim, J. Elle, A. Sushkov, G. Jenkins, H. Milchberg, M. Fuhrer, and H. Drew, "Dual-gated bilayer graphene hot-electron bolometer," *Nature Nanotechnology*, vol. 7, no. 7, pp. 472–478, 2012.
- [3] . Sakolu, J. S. Tyo, M. M. Hayat, S. Raghavan, and S. Krishna, "Spectrally adaptive infrared photodetectors with bias-tunable quantum dots," *Journal of the Optical Society of America B*, vol. 21, no. 1, pp. 7–17, 2004. [Online]. Available: <http://josab.osa.org/abstract.cfm?URI=josab-21-1-7>
- [4] P. Li, X. Yang, T. W. W. Ma, J. Hanss, M. Lewin, A.-K. U. Michel, M. Wuttig, and T. Taubner, "Reversible optical switching of highly confined phononpolaritons with an ultrathin phase-changematerial," *Nature Materials*, vol. 15, p. 870, 2016. [Online]. Available: <http://dx.doi.org/10.1038/nmat4649>
- [5] N. I. Zheludev and E. Plum, "Reconfigurable nanomechanical photonic metamaterials," *Nature nanotechnology*, vol. 11, no. 1, p. 16, 2016.
- [6] Y. Yao, M. A. Kats, R. Shankar, Y. Song, J. Kong, M. Loncar, and F. Capasso, "Wide wavelength tuning of optical antennas on graphene with nanosecond response time," *Nano letters*, vol. 14, no. 1, pp. 214–219, 2013.
- [7] M. D. Goldflam, Z. Fei, I. Ruiz, S. W. Howell, P. S. Davids, D. W. Peters, and T. E. Beechem, "Designing graphene absorption in a multispectral plasmon-enhanced infrared detector," *Optics Express*, vol. 25, no. 11, pp. 12400–12408, 2017. [Online]. Available: <http://www.opticsexpress.org/abstract.cfm?URI=oe-25-11-12400>
- [8] B. Olson, C. Grein, J. Kim, E. Kadlec, J. Klem, S. Hawkins, and E. Shaner, "Auger recombination in long-wave infrared inas/inasb type-ii superlattices," *Applied Physics Letters*, vol. 107, no. 26, p. 261104, 2015.
- [9] Y. Aytac, B. Olson, J. Kim, E. Shaner, S. Hawkins, J. Klem, M. Flatt, and T. Boggess, "Effects of layer thickness and alloy composition on carrier lifetimes in mid-wave infrared inas/inasb superlattices," *Applied Physics Letters*, vol. 105, no. 2, p. 022107, 2014.
- [10] G. Dyer, X. Shi, B. Olson, S. Hawkins, J. Klem, E. Shaner, and W. Pan, "Far infrared edge photoresponse and persistent edge transport in an inverted inas/gasb heterostructure," *Applied Physics Letters*, vol. 108, no. 1, p. 013106, 2016.
- [11] M. D. Goldflam, E. A. Kadlec, B. V. Olson, J. F. Klem, S. D. Hawkins, S. Parameswaran, W. T. Coon, G. A. Keeler, T. R. Fortune, A. Tauke-Pedretti, J. R. Wendt, E. A. Shaner, P. S. Davids, J. K. Kim, and D. W. Peters, "Enhanced infrared detectors using resonant structures combined with thin type-ii superlattice absorbers," *Applied Physics Letters*, vol. 109, no. 25, p. 251103, 2016. [Online]. Available: <http://aip.scitation.org/doi/abs/10.1063/1.4972844>
- [12] D. R. Rhiger, "Performance comparison of long-wavelength infrared type ii superlattice devices with hgcdte," *Journal of electronic materials*, vol. 40, no. 8, pp. 1815–1822, 2011.
- [13] C. Grein, J. Garland, and M. Flatte, "Strained and unstrained layer superlattices for infrared detection," *Journal of electronic materials*, vol. 38, no. 8, pp. 1800–1804, 2009.
- [14] O. Gravrand, J. Wlassow, and L. Bonnefond, "A calibration method for the measurement of ir detector spectral responses using a ftir spectrometer equipped with a dtgs reference cell," in *High Energy, Optical, and Infrared Detectors for Astronomy VI*, vol. 9154. International Society for Optics and Photonics, 2014, Conference Proceedings, p. 91542O.